Chapter 3

Experimental Setup

Here, the experimental equipment is presented, the newly developed polarization shaping-capable setups demand a more detailed treatment and will be separately introduced in the later chapters.

3.1 Molecular beam apparatus

The molecules investigated throughout this work have to be prepared in a special environment not to interact with each other. The goal is to set them up in a way that their behavior can be comprehended as much as possible, which requires a source where every cluster has the same starting conditions. A molecular beam is a way of obtaining vibrationally cool, but translationally hot species relative to the laboratory frame [53], and is otherwise often employed for molecular epitaxy [54].

As many in-detail descriptions of the used molecular beam apparatus (Fig. 3.1) are available [36, 55, 56], only a brief summary will be given. The alkali clusters originate from an adiabatic co-expansion of the respective vapors (heated inside a small cylindrical oven with a small nozzle of about 70 μm) into the vacuum, which is driven by argon as a carrier gas. After skimming the beam, the clusters enter the detection chamber where they interact with the femtosecond laser. The ionized species are focused towards the entrance of the mass selector using electrostatic lenses. The mass filter, made from four parallel, cylindrical rods generates a quadrupole field which can be adjusted that only the selected mass has a stable trajectory and reaches the secondary electron multiplier. The mass resolution $m/\Delta m > 200$ is high enough to distinguish between $^{39,39}K_2$ and $^{39,41}K_2$ and also between $^{23}Na^{39}K$ and $^{23}Na^{41}K$.

A rotary vane pump (RVP) and a roots pump (RP) provide the pre-vacuum with a pressure of roughly 10^{-3} mbar. The oven chamber is pumped by a 3000 l/s diffusion oil pump (DP) which keeps the pressure still below 10^{-3} mbar even when the molecular beam is present. To prevent contamination of the chamber with oil, a cooled trap (CT) is placed between the DP and the oven chamber. The detection chamber is evacuated by a turbo molecular pump (TP) which keeps it between 2 and 5×10^{-6} mbar during the measurements. Typical oven temperatures are around 650°C, typical argon pressures about 2.5 bar and the resulting NaK and K_2 dimers have vibrational temperatures below 50 K and rotational temperatures below 10 K, leaving mostly the ground state populated [57].

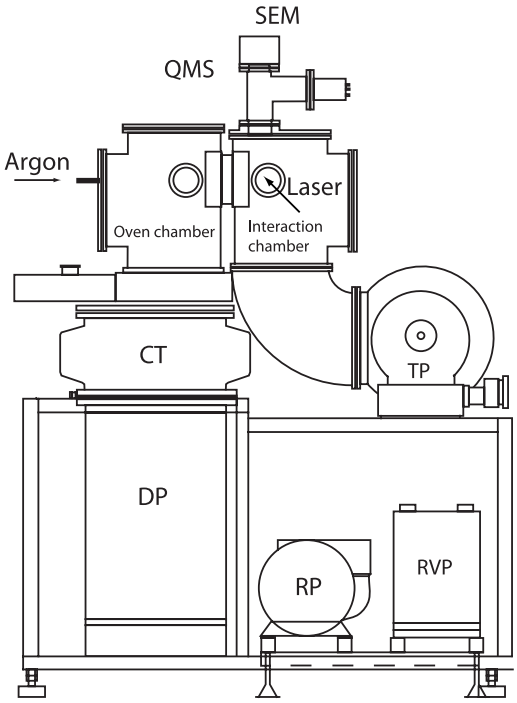

Figure 3.1: Molecular beam apparatus showing the vacuum pumps, the oven chamber (left top), interaction chamber (right top) and the mass spectrometers (QMS) with the secondary electron multiplier (SEM).

3.2 Laser systems and pulse detection

The laser systems used throughout this work were on the one hand an 80 MHz Ti:sapphire oscillator (Spectra Physics Tsunami), pumped by a Spectra Physics Millennia X (delivering about 10 nJ per pulse and an intensity of about 1 GW/cm^2 when focused to approx. 100 μm), and a new system that provided kHz pulses with up to several hundred times higher pulse energies. The reason for the switch (Coherent RegA 9050 Ti:sapphire amplifier, seeded by a Coherent Mira) which provides a 100-250 kHz repetition rate was the requirement not to irradiate one molecule more than once while passing through the interaction zone. Also, the peak intensities should not be as high that they would require other descriptions than the perturbative picture [56], allowing the experiment still to be treated in the linear regime where non-resonant multi-photon processes are unlikely [58]. If pulses with significantly higher pulse energies were employed, possible interference effects in non-resonant multi-photon processes would have to be considered [59].

Apart from the pulse energies, also the typical bandwidths were different, spanning from 6 - 15 nm for the Tsunami to 22 - 35 nm for the RegA, which has to be kept in mind when comparing the results obtained with the two setups.

3.3 Pulse shaper setup for linearly polarized pulses

Throughout this work, three different pulse shaper setups were employed, two of them were newly developed during the time of this work together with M. Plewicki [28], and will be described in Chapters 7 and 8.

The standard 4f-setup utilized for linear pulse shaping originated from the "zero-dispersion compressor" setup [60]. It dissolves a broadband input pulse and separates the frequency components in a Fourier plane which lies in between two gratings

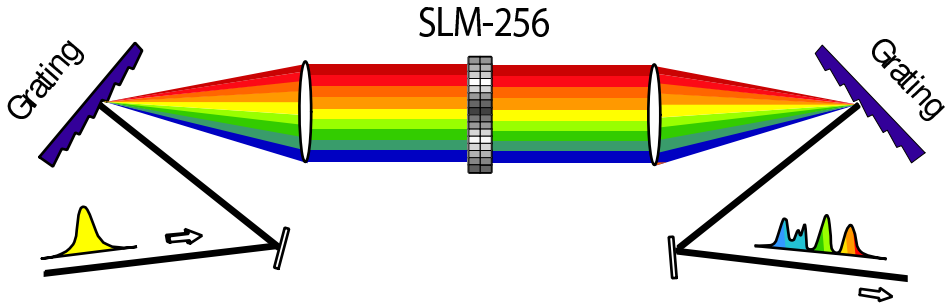

Figure 3.2: Illustration of a 4f pulse shaper. The distances grating-lens-modulator-lens-grating are all of the focal length f. The liquid crystal modulator is situated in the Fourier plane of the setup.

and two lenses that are arranged symmetrically with distances of exactly the focal length f of the lenses. Within this Fourier plane[1], a femtosecond laser pulse can be manipulated in various ways and by various devices, for example static phase masks [62, 63] or acousto-optical modulators [64, 65].

Fig. 3.2 depicts the 4f-setup [66] used for pulse shaping with linearly polarized pulses employing the SLM-256 modulator [67], whereby SLM means Spatial Light Modulator. On entering the first grating, the broadband pulse is diffracted, collimated by a cylindrical lens (f=20 cm) and then focused to the Fourier plane, where every frequency component corresponds to a different spatial position. The spot size due to the finite beam size can be calculated [37, 68] by

$$w_0 = \frac{\lambda f}{\pi w_{in}} \tag{3.1}$$

(where w_{in} is the input beam diameter) and amounts[2] to about a quarter of the used SLM's pixel width of 100 μm.

Side-effects. A number of other effects has to be taken into account when an accurate picture of the output of a liquid crystal modulator is desired: Quantization effects due of the discretization of the pixel mask with the effective mask function [37]

$$\tilde{M}(\omega) = \left(\tilde{H}(\omega) \cdot \sum_{n=-N/2}^{(N/2)-1} \delta(\omega - n\delta\omega)\right) * rect\left[\frac{\omega}{\delta\omega}\right] \tag{3.2}$$

might become an issue, whereby *rect* is a square wave function, convoluted ($*$) with the Dirac delta-function, $\delta\omega$ the frequency width of one pixel (assumed constant for this calculation), n the pixel number, N the total number of pixels, and $\tilde{H}(\omega)$ the complex filter function. The inverse Fourier transform of the mask function determines prominent points in time for so-called replica-pulses [36, 37]. From the discretization $\delta\omega$, the "shaping window" Δt can be estimated [69] to be $\Delta t = 2\pi/\delta\omega$. Other effects are "blind spots" and smoothing effects due to the gaps between the pixels (2 μm for the SLM 640) and diffraction effects at the pixel edges, leading

[1] an alternative approach without Fourier plane can be found in Ref. [61]
[2] for 770 nm central wavelength, f=20 cm, and 6 mm beam diameter

Pixel elements per mask	640
Pixel Height	5.0 mm
Pixel Pitch	100 μm $\pm$ 0.005 μm
Interpixel Gap	2.0 μm
Intermask Alignment	$\pm$ 2.0 μm
Intermask Separation	1.02 mm
Transmission (excl. polarizer)	$>$ 94 %
Spectral Range	488 - 900 nm / 400-1620 (derated transm.)
Coating Losses	$<$ 3 %
Damage Threshold	200 μJ/cm^2 (890 nm, 50 fs, 1kHz)
Response Time	35 ms (2 π at 900 nm)
Drive Resolution	12 bit (2.44 mV steps)
Frame Buffers	32
Interface	USB 1.1, 460800 bit/s data rate

Table 3.1: Technical specifications of the SLM-640, taken from [38].

to a space-time coupling of the produced waveforms [70]. If spread over a larger wavelength range, the fact that the frequencies are not linearly distributed along the Fourier plane also have to be taken into account [70, 71].

Phase and amplitude modulation. As stated in Eq. 2.21, a spectral field $E(\omega)$ can be generated in phase and amplitude using a double-array modulator, arranged with optical axes aligned $\pm 45°$. It enacts the respective array retardances $\phi_a(\omega)$ and $\phi_b(\omega)$. When adding a polarizer in x-direction after the pulse shaper the output field will be[3]

$$E_{out}^{ph+amp}(\omega) = E_{in}(\omega) \cdot e^{\frac{i}{2}[\phi_a(\omega)+\phi_b(\omega)]} \cdot \cos\frac{\phi_a(\omega) - \phi_b(\omega)}{2} \tag{3.3}$$

whereby $E_{in}(\omega)$ is the linearly polarized input pulse including the fast oscillating part. For the following, the "difference-phase" will be defined as $\Delta\phi = \phi_a - \phi_b$ and as frequency dependent transmission, $T(\omega) = \cos^2[\Delta\phi(\omega)/2]$ will be regularly employed.

3.3.1 SLM-640 prototype

For the chapters utilizing polarization shaping (Chapters 7 & 8), a prototype model of the SLM-640 [38] from CRi Inc. (Cambridge Research and Instrumentation) was used. It was one of the first commercially manufactured dual array modulators with 2×640 pixels.

An excerpt from the technical specifications is provided by Table 3.1. Apart from the greater number of pixels and an increased array width of 6.4 cm, it is similar in most aspects to the SLM-256 [67] employed for Chapters 4, 5, and 6.

The unit was originally shipped with a 115.2 kbit/s RS-232 serial interface which would have seriously slowed down experiments compared to the SLM-256, and had

[3] a derivation implementing Jones calculus will be given in Sec. 7.1.1

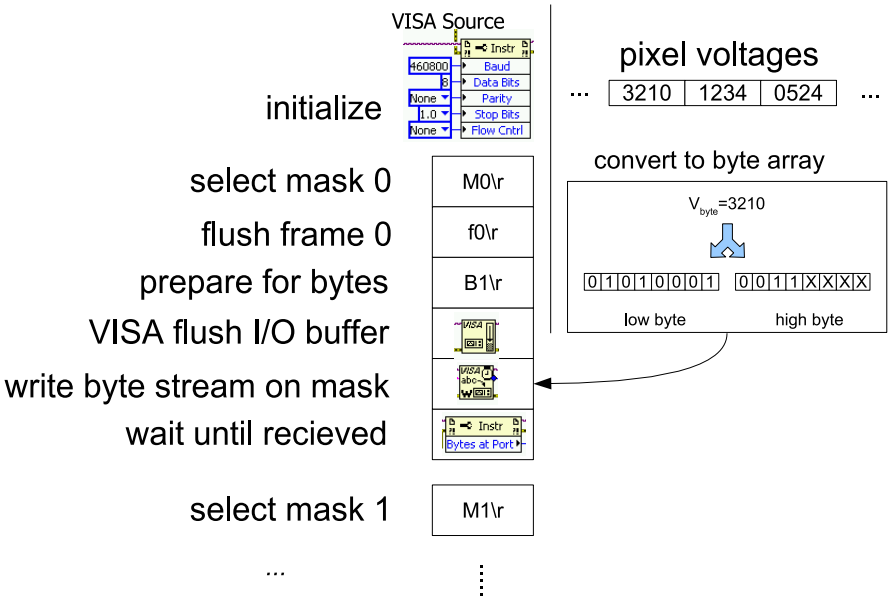

Figure 3.3: Sketch of the implemented Labview/VISA driver for the SLM-640.

other issues[4]. The final unit was shipped with an improved USB interface that was capable of effectively delivering a data rate of 460 kbit/s. The data processing is performed by two high-speed DSP processors. The drive level per pixel is sampled by 12 bits, with a voltage of $V_i = V_{ref} \times (D_i/4096)$ where V_i is the voltage at pixel i and D_i its digital drive level, and V_{ref}=10 V is the reference voltage.

A fast and reliable interface driver for the USB SLM-640 model is presented in Fig. 3.3. It is incorporated in the Labview^{TM}development system using the NI-VISA language. The connection to the USB device is handled via a virtual serial COM port, which is addressed by Labview-VISA. The dual mask is addressed sequentially with a set of ASCII commands. To transmit a specific voltage array to the shaper, the serial VISA instrument is first configured and initialized with the connection's settings (Fig. 3.3 top). First, one of the two arrays masks is selected, then its frame buffer flushed, finally the `B` command prepares the shaper for receiving a bytestream which has to be recoded to a 16-bit format, where only 12 bit carry information and the upper 4 bit are discarded (marked by the X on the top right of Fig. 3.3). After flushing the I/O buffer, the bytestream can be sent, and after confirming reception, the second mask can be addressed in a similar fashion.

3.4 Pulse detection

The pulses were characterized by an Ocean Optics fiber spectrometer which records the spectral intensity, which is $I(\omega) \propto |E(\omega)|^2$. The limited spectral resolution, which can be incorporated by convoluting (marked by $*$) with the resolution

[4]The first and second prototype delivered had, for example, serious issues with leak currents between the pixels and/or arrays.

function $I_r(\omega)$ is

$$|E'_{res}(\omega)|^2 = |E(\omega)|^2 * I_r(\omega). \tag{3.4}$$

For the time-domain, the sum-frequency-generated-cross-correlations (abbreviated SFG-CC) uses light which originates from two non-collinearly overlapped pulses in a non-linear BBO-crystal. The pulses from the Tsunami were recorded with a photodiode and a photomultiplier; for the kHz RegA system, a boxcar averager was used instead of the multiplier.

The SFG-CC can be calculated by performing the correlation of the pulse form to be measured with the known reference pulse's intensity as

$$I_{SFG}(\tau) = \int_{-\infty}^{+\infty} |E(t)^*|^2 \cdot |E_r(t-\tau)|^2 dt. \tag{3.5}$$

Furthermore, XFROG [72] (from Frequency-Resolved Optical Gating) traces were aquired which can be calculated from the electric field $E(t)$ of the target and reference pulse $E_r(t)$ as

$$I_{XFROG}(\omega,\tau) = \left| \int_{-\infty}^{\infty} E(t) E_r(t-\tau) e^{-i\omega t} dt \right|^2. \tag{3.6}$$

The employed pulse detection for polarization shaped pulses will be described in Sec. 7.4.1.